

Sliced Surface Generation Mechanism of Unidirectional Glass Fiber-Reinforced Plastic by Multi-Wire Sawing

Satoshi Sakamoto, Tomohito Fujioka, and Liu Jiayu
College of Education, Yokohama National University, Yokohama, Japan
Email: {sakamoto-satoshi-tv, fujioka-tomohito-ws, liu-jiayu-bz}@ynu.jp

Mitsugu Yamaguchi
Institute of Industrial Science, the University of Tokyo, Kashiwa, Japan
Email: ymitsugu@iis.u-tokyo.ac.jp

Yasuo Kondo
Graduate School of Science and Engineering, Yamagata University, Yonezawa, Japan
Email: kondo@yz.yamagata-u.ac.jp

Kenji Yamaguchi
Department of Mechanical Engineering, Yonago National College of Technology, Yonago, Japan
Email: yama@yonago-k.ac.jp

Abstract—Anisotropic materials represented by fiber-reinforced plastic (FRP) are widely used in various fields because of their high specific strength. However, the cutting resistance greatly fluctuates because anisotropic materials have strength anisotropy. Therefore, the field of cutting has been studied for a long time now. Meanwhile, several research reports on abrasive grain processing have been presented, but many unknown points exist at present. In this study, we investigated the generation mechanism of the sliced surface when slicing an anisotropic material using an electrodeposited diamond wire tool. Unidirectional glass fiber-reinforced plastic (GFRP) was used as the work material. Consequently, it was found that the slicing rate does not depend on the slicing angle or slicing area. The accuracy of the sliced surface roughness and the wafer thickness degraded as the slicing angle increased. The generation mechanism of the sliced surface differs depending on the slicing system. In other words, in the free abrasive grain system, it becomes the generation mechanism of the sliced surface mainly by microfractures. In contrast, in the fixed abrasive grain system, the generation mechanism of the sliced surface is mainly by microcutting in the ductility mode.

Index Terms—slicing, multi-wire saw, anisotropic materials, glass fiber-reinforced plastic, electrodeposited diamond wire tool, surface generation mechanism

I. INTRODUCTION

Recently, various functional materials have been attracting attention and have been developed. Anisotropic

materials, represented by fiber-reinforced plastic (FRP), are used in a wide range of fields, from consumer goods (e.g., sporting goods) to military goods (e.g., aircraft), because of their superior mechanical properties (e.g., high specific strength) [1].

FRP parts are generally manufactured using the near-net-shape method. Therefore, FRP requires little machining after molding. However, secondary processing, such as cutting and drilling, is required to produce various parts. Abrasive machining (e.g., grinding) may be required to produce high-precision parts.

Anisotropic materials are difficult to cut because they have strength anisotropy, and the machining resistance when cutting an anisotropic material greatly fluctuates. In addition, burrs and delamination tend to occur. Therefore, for a long time, there has been ongoing research in the field of cutting [2, 3], with special focus on high-precision cutting in the recent years [4–7]. In contrast, only a few research reports have focused on the machinability of anisotropic materials in the field of abrasive machining [8, 9]. However, this field has many unknown points at present.

Multi-wire sawing is one of the excellent methods used to slice semiconductors and optical materials with high-precision [10]. The free abrasive grain system and the fixed abrasive grain system are used in slicing with a multi-wire saw. Here, we investigate the machining characteristics of FRP by the free abrasive grain system [11–14]. The results of this study showed that the orientation angle of the reinforced fiber greatly influences the generation of the machined surface. The main objective of this study is to clarify the generation

mechanism of the sliced surface of anisotropic materials by the fixed abrasive grain system. The previous report clarified the wear characteristics of electrodeposited diamond wire tools during FRP slicing [15]. This paper describes the fundamental sliced surface generation mechanism of unidirectional reinforced FRP using an electrodeposited diamond wire tool.

II. EXPERIMENTAL PROCEDURE

Fig. 1 shows a schematic illustration of the experimental apparatus. The multi-wire saw used herein was a reciprocating-type wire saw. In this multi-wire saw, one drum simultaneously controlled the feeding and rewinding of the wire tool.

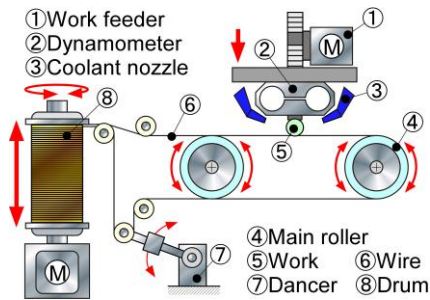


Figure 1. A schematic illustration of the experimental apparatus (multi-wire saw for the slicing experiments).

Table I summarizes the main experimental conditions and materials used in this study. Unidirectional glass fiber-reinforced plastic (GFRP) with a diameter of 20 mm was used as the work material. The reinforced fibers contained in the GFRP had a diameter of 25 μm and a filling rate of 60–70 vol.%. An electrodeposited diamond wire tool with a core diameter of 100 μm and an outer diameter of 143 μm was used in the slicing experiments. The particle size of the electrodeposited diamond abrasives was 30–40 μm, the tension given to the wire tool was 14.6 N, the running speed of the wire tool was 200 m/min, and the feed rate of the work material was 0.6 mm/min.

TABLE I. MAIN EXPERIMENTAL CONDITIONS AND MATERIALS USED

Wire	Electrodeposited diamond wire tool	
	Abrasives	Diamond
	Grain size	30–40 μm
	Material of the core wire	SWRS82A
	Diameter of the core wire	100 μm
	Outer diameter	143 μm
	Breaking strength	36.9 N
	Running speed	200 m/min
	Tension	14.6 N
Work	Unidirectional reinforced GFRP	
	Outer diameter	20 mm
	Diameter of the reinforced fiber	25 μm
	Filling rate of the reinforced fiber	60–70 vol.%
Coolant	Feed rate	0.6 mm/min
	Solution-type	
	Supply amount	10 mL/min

Fig. 2 shows the angle between the orientation direction of the reinforced fibers and the running direction of the wire tool. The angle formed by the running direction of the wire tool and the reinforced fiber is referred to herein as the slicing angle. This slicing angle is defined as 0° when the running direction of the wire tool and the orientation of the reinforced fibers are parallel. Conversely, the slicing angle is defined as 90° when they are orthogonal.

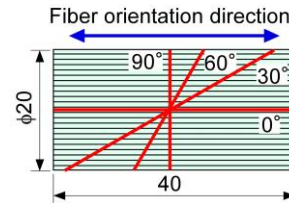


Figure 2. Definition of the slicing angle.

Fig. 3 shows a schematic illustration of the fracture surface of the reinforced fibers appearing on the sliced surface. When the slicing angle was 0°, the reinforced fibers appeared in the sliced surface with almost no cutting because they were sliced in parallel with the reinforced fibers. When the slicing angle was 30°, the reinforced fibers appeared in an elliptical shape with a minor axis of 25 μm and a major axis of 50 μm. The major axis of the ellipse became maximum when the slicing angle was 30°. In other words, the area of the fracture surface of the reinforced fibers was maximized. When the slicing angle was 60°, the reinforced fibers appeared in an elliptical shape with a minor axis of 25 μm and a major axis of 29 μm. When the slicing angle was 90°, the orientation of the reinforced fiber was orthogonal to the slicing direction. Therefore, the reinforced fibers appeared in the sliced surface in a circle with a diameter of 25 μm.

Table II shows the relationship between the slicing angle and the slicing area. Naturally, the slicing area greatly changed as the slicing angle changed (i.e., the slicing area decreased as the slicing angle increased). The slicing area differed by 2.5 times or more when the slicing angle was 0° and 90°.

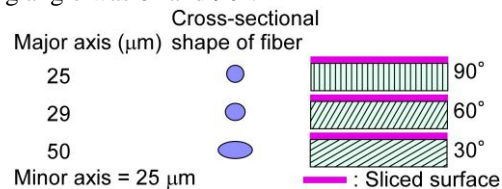


Figure 3. A schematic illustration of the fracture surface of the reinforced fibers appearing on the sliced surface.

TABLE II. RELATIONSHIP BETWEEN THE SLICING ANGLE AND THE SLICING AREA

Slicing angle (°)	Slicing area (mm ²)
0	800
30	628
60	364
90	314

Fig. 4 shows the measurement position of the sliced surface roughness and the wafer thickness. The sliced surface roughness and the wafer thickness were measured at three points: initial, middle, and later stages of slicing (Fig. 4). The measurements were taken at the center of the work material at any slicing angle. The evaluation length in the surface roughness measurement was 5 mm, and the cutoff was 0.8 mm. The measurement was performed thrice at three points, and the average value was taken as the measurement value.

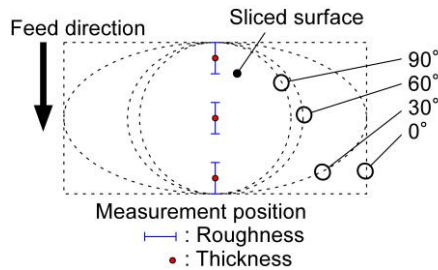


Figure 4. Definition of the measurement points.

III. EXPERIMENTAL RESULTS AND DISCUSSION

A. Influence of the Slicing Angle on the Slicing Rate

Fig. 5 shows the relationship between the slicing angle and the slicing rate. The broken line in the figure denotes the feed rate of the work material, which is 0.6 mm/min. The slicing area greatly varied depending on the slicing angle (Table II), but no significant difference in the slicing rate was observed. The slicing rate was slightly slower than the feed rate of the work material, but it showed a nearly constant value, regardless of the slicing angle. In other words, the slicing rate did not depend on the slicing angle or the slicing area. The excellent machinability of the GFRP used as the work material herein was one of the reasons why the influence of the increase and decrease in the slicing area did not appear to be remarkable. The slicing rate did not decrease even if the slicing area increased because the GFRP was easily sliced; hence, the influence of the slicing area did not appear to be remarkable. Therefore, the increase or decrease in the slicing area caused by the change in the slicing angle had no significant effect on the slicing characteristics.

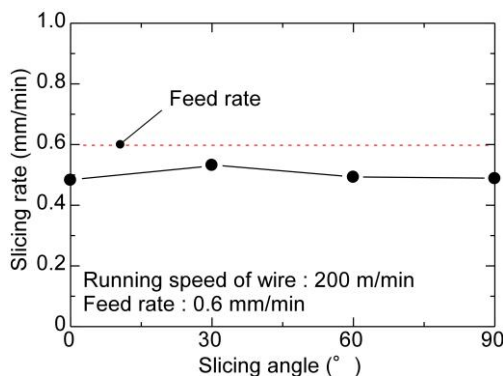


Figure 5. Relationship between the slicing angle and the slicing rate.

B. Influence of the Slicing Angle on the Surface Roughness

Fig. 6 shows the relationship between the slicing angle and the sliced surface roughness. The white circle indicates the arithmetic average roughness (R_a), whereas the black circle indicates the maximum height (R_z). The sliced surface roughness tended to degrade as the slicing angle increased. The arithmetic average roughness (R_a) and the maximum height (R_z) showed the same tendency. In the free abrasive grain system (e.g., slicing using slurry), when the cross-sectional area of the reinforced fiber appearing on the sliced surface was larger, the sliced surface roughness tended to deteriorate [11]. Namely, the sliced surface roughness greatly degraded when the slicing angle was 30°. However, the same tendency as in the result of the free abrasive grain system was not obtained in the fixed abrasive grain system using the electrodeposited diamond wire tool. The sliced surface roughness did not depend on the cross-sectional area of the reinforced fibers that appeared in the sliced surface and tended to deteriorate as the slicing angle increased.

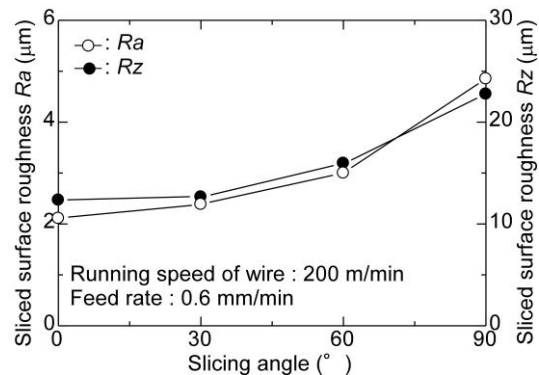


Figure 6. Relationship between the slicing angle and the surface roughness.

C. Observation of the Sliced Surfaces

The tendencies of the sliced surface roughness by the free abrasive grain system using slurry and the sliced surface roughness by the fixed abrasive grain system using the electrodeposited diamond wire tool were greatly different. Therefore, a comparative observation of the sliced surfaces was performed. In the free abrasive grain system, a wire tool with a diameter of 160 μm was used. The particle size of the abrasives in the slurry was 11.5 μm .

Fig. 7 presents an example of a sliced surface when the slicing angle was 0°. Specifically, (A) denotes a sliced surface by the fixed abrasive grain system, whereas (B) depicts a sliced surface by the free abrasive grain system. Focusing on the reinforced fiber, the scratch marks of the electrodeposited diamond wire tool can be confirmed on the sliced surface by the fixed abrasive grain system. By contrast, microfractures can be confirmed in the reinforced fibers appearing on the sliced surface by the free abrasive grain system.

Figs. 8–10 show examples of sliced surfaces at slicing angles of 30°, 60°, and 90°, respectively.

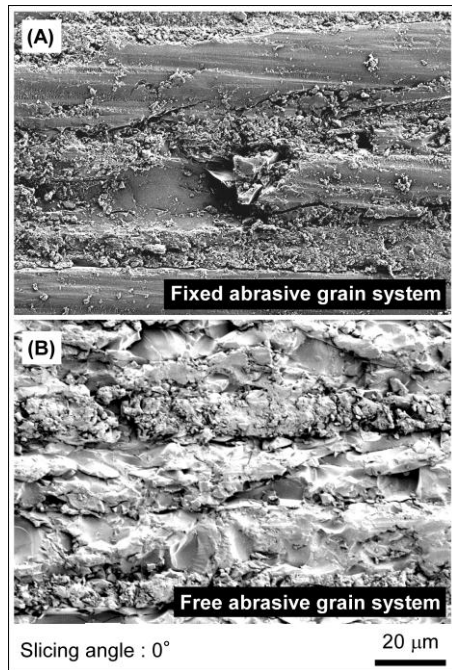


Figure 7. Example of a sliced surface at a slicing angle of 0°.

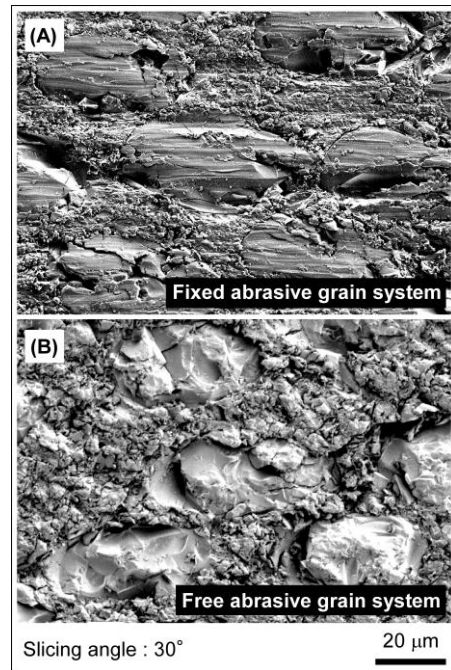


Figure 8. Example of a sliced surface at a slicing angle of 30°.

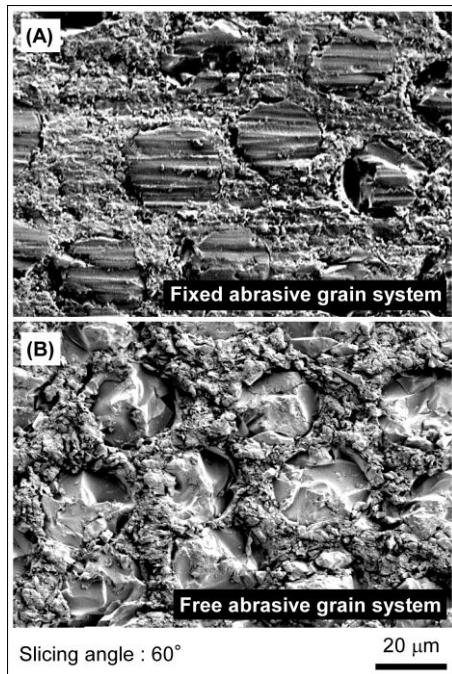


Figure 9. Example of a sliced surface at a slicing angle of 60°.

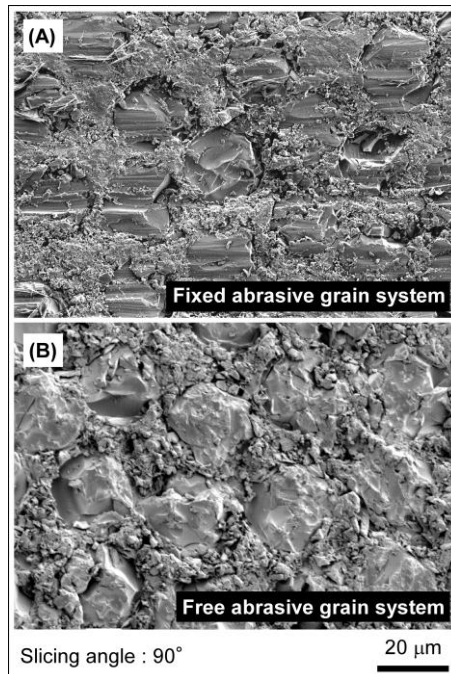


Figure 10. Example of a sliced surface at a slicing angle of 90°.

The characteristics of the sliced surface of the fixed abrasive grain system and the free abrasive grain system were largely different because the generation mechanism of the sliced surface was significantly different. In other words, the sliced surface generation mechanism by the free abrasive grain system was mainly based on micro-brittle fractures. In contrast, in the surface generation mechanism by the fixed abrasive grain system, microcutting in the ductile mode was the main body.

D. Influence of the Slicing Angle on the Wafer Thickness

Fig. 11 shows the relationship between the slicing angle and the wafer thickness. The arrangement pitch of the electrodeposited diamond wire tool in the experimental equipment (multi-wire saw) was 2 mm. The outermost diameter of the electrodeposited diamond wire tool used herein was 143 μm. Therefore, the assumed wafer thickness was approximately 1.86 mm. The wafer thickness deviated from the assumed thickness as the slicing angle increased. In addition, the wafer thickness variation tended to increase.

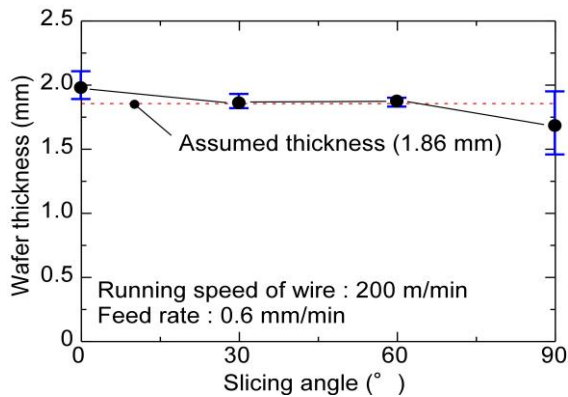


Figure 11. Relationship between the slicing angle and the wafer thickness.

IV. CONCLUSIONS

In this study, we experimentally investigated the fundamental surface generation mechanism when unidirectional GFRP was sliced using an electrodeposited diamond wire tool. As a result, it was found that the slicing rate did not depend on the slicing angle. The sliced surface roughness and the accuracy of the thickness of the wafer tended to deteriorate as the slicing angle increased. The generation mechanism of the sliced surface by the wire tool was largely different between the free abrasive grain system and the fixed abrasive grain system. The sliced surface generation mechanism by the free abrasive grain system was mainly based on micro-brittle fractures. In contrast, in the surface generation mechanism by the fixed abrasive grain system using the electrodeposited diamond wire tool, microcutting in the ductile mode was the main body.

CONFLICT OF INTEREST

The authors declare no conflict of interest.

ACKNOWLEDGMENT

We would like to thank Mr. Masaya Gemma (Keio Futsubu School) and the Instrumental Analysis Center of Yokohama National University for their support and cooperation. Additionally, part of this work was supported by JSPS KAKENHI Grant Number 16K06005.

REFERENCES

- [1] C. Soutis, "Carbon fiber reinforced plastics in aircraft construction," *Mater. Sci. Eng. A*, vol. 412, pp. 171-176, December 2005.
- [2] H. Takeyama, N. Iijima, S. Noguchi, and Y. Kagami, "Study on cutting mechanism of composite material GFRP," *J. Jpn. Soc. Precis. Eng.*, vol. 53, pp. 1447-1452, September 1987.
- [3] X. Wang, K. Nakayama and M. Arai, "Investigation on cutting of fiber reinforced composite material—Improvement of surface finish in cutting GFRP—," *J. Jpn. Soc. Precis. Eng.*, vol. 55, pp. 709-714, April 1989.
- [4] I. S. N. V. R. Prasanth, D. V. Ravishankar, M. Manzoor Hussain, C. M. Badiganti, V. K. Sharma, and S. Pathak, "Investigations on performance characteristics of GFRP composites in milling," *Int. J. Adv. Manuf. Technol.*, vol. 99, pp. 1351-1360, November 2018.
- [5] D. Rychkov, D. Lobanov, and A. Kuznetsov, "Achieving high quality surface of laminated glass-reinforced plastics during

- milling," *MATEC web of Conf.*, vol. 224, article no. 01040, October 2018.
- [6] Y. Kondo and S. Sakamoto, "A damage-free machining method for CFRP without feedback control systems," *Int. J. of Automation. Technol.*, vol. 10, no. 3, pp. 318-323, May 2016.
- [7] G. Liu, H. Chen, Z. Huang, F. Gao, and T. Chen, "Surface quality of staggered PCD end mill in milling of carbon fiber reinforced plastics," *Appl. Sci.*, vol. 7, issue 2, article no. 199, February 2017.
- [8] S. Teraoka, K. Ishikawa, T. Nakagawa, and S. Ohba, "Study on abrasive wear process of CFRP in vibrating environment," *Trans. of the Jpn. Soc. of Mech. Eng., Ser. C*, vol. 61, No. 581, pp. 180-185, January 1995.
- [9] S. Teraoka, K. Ishikawa, T. Nakagawa, and K. Ohta, "Study on abrasive wear characteristics of CFRP in vibrating environment—Wear characteristics under three-body conditions—," *Trans. of the Jpn. Soc. of Mech. Eng., Ser. C*, vol. 63, No. 611, pp. 2464-2469, July 1997.
- [10] H. Wu, "Wire sawing technology: A state-of-the-art review," *Precis. Eng.*, vol. 45, pp. 1-9, January 2016.
- [11] S. Sakamoto, M. Yamaguchi, Y. Kondo, K. Yamaguchi, and A. J. Nomura, "Surface characteristics produced by multi-wire sawing of GFRP," *Key Eng. Mater.*, vol. 625, pp. 597-602, August 2014.
- [12] M. Yamaguchi, S. Sakamoto, Y. Kondo, K. Yamaguchi, and K. Hayashi, "Lapped surface generation mechanism of unidirectional fiber reinforced composite materials," *J. Jpn. Soc. Precis. Eng.*, vol. 81, pp. 668-672, July 2015.
- [13] M. Yamaguchi, S. Sakamoto, Y. Kondo, K. Yamaguchi, and H. Usuki, "Study on slicing characteristics of fiber reinforced plastics by multi-wire saw," presented at the 9th International Conference on History of Mechanical Technology and Mechanical Design (ICHMTMD2012), Tainan, Taiwan, March 23-25, 2012.
- [14] S. Sakamoto, M. Yamaguchi, A. Nomura, Y. Kondo, K. Yamaguchi, and T. Yakou, "Influence of orientation angle of fiber on sliced surface of GFRP," presented at the 5th KSME-JSME Joint International Conference on Manufacturing, Machine Design and Tribology (ICMDT2013), Busan, Korea, May 22-25, 2013.
- [15] M. Gemma, K. Hayashi, S. Sakamoto, Y. Kondo, K. Yamaguchi, and T. Fujita, "Fundamental machinability of composite materials using wire tool electrodeposited diamond grains," presented at the JSPE Autumn Meeting, Ibaraki, Japan, September 6-8, 2016.

Copyright © 2020 by the authors. This is an open access article distributed under the Creative Commons Attribution License ([CC BY-NC-ND 4.0](https://creativecommons.org/licenses/by-nc-nd/4.0/)), which permits use, distribution and reproduction in any medium, provided that the article is properly cited, the use is non-commercial and no modifications or adaptations are made.



Satoshi Sakamoto's laboratory of Yokohama National University.

Satoshi Sakamoto received his doctorate from Kanazawa University, Japan in 1997. Now he is a professor at Yokohama National University. His current research interests include precision machining of hard and brittle materials. He is a member of the Japan society for precision engineering, the Japan society of mechanical engineers, and the Japan society for abrasive technology. Tomohito Fujioka and Liu Jiayu are student in Satoshi



Mitsugu Yamaguchi received the Dr. Eng. degree in 2016 from Ibaraki University. He is currently a project researcher at Institute of Industrial Science, The University of Tokyo. His current research interests include laser sintering of metal nanoparticles for metal substrates and cutting of difficult-to-cut materials.



Yasuo Kondo received his Ph.D Degree in 1994 from Osaka University. Now he is a professor of Graduate School of Science and Engineering, Yamagata University. His research interests include manufacturing system, On-line monitoring system for machining operation and Engineering education.



Kenji Yamaguchi received the Ph.D degree in 2002 from Tottori University. His current position is a professor of the Department of Mechanical Engineering, Yonago National College of Technology. His research interests include an effective succession of technicians' skill and a monitoring system for cutting fluids condition.